Mon. Not. R. Astron. Soc. **000**, 1–10 (0000) Printed 4 May 2011 (MN LATEX style file v2.2)

# Dark halo mass function in a prescribed spherical host perturbation – Press–Schechter theory with statistical constraints

E. P. Kurbatov[1⋆]
[1]*Institute of Astronomy, 48 Pyatnitskaya St., Moscow, 119017, Russia*

4 May 2011

**ABSTRACT**
Here proposed a modification of the Press–Schechter theory allowing for the presence of a host density perturbation – host halo or void. The perturbation is accounted as statistical constraints in a form of linear functionals of the random overdensity field. Deviation of the background density within perturbation is interpreted in a pseudo-cosmological sense. Resulting mass function of sub-haloes depends on the perturbation parameters: its mean overdensity, spatial scale, and spatial momenta of higher orders. Applications of the theory to superclusters, voids and bias problem are briefly observed. In its present form, the theory can describe the clustering properties of sub-haloes inside a non-virialized host only. Possible fix of this drawback is also discussed.

**Key words:** large-scale structure of Universe – galaxies: luminosity function, mass function

## 1 INTRODUCTION

The theory of Press and Schechter originated as a semi-analytical approach to describing the evolution of the mass function of dark haloes. Today this theory, together with its modifications, perhaps the only one that, using some reservations, most closely matches observations and numerical modeling for the widest mass range of dark haloes, down to the resolution limit of numerical runs. The reservations of the theory concerned to its main provisions:

– reinterpretation of halo merging as a random walk process allowed to complete the construction of the theory with a mass function of Press and Schechter (Bond et al. 1991);
– Benson et al. (2005) showed, in the original theory the merger rate, or the merger kernel, in terms of Smoluchowski equation, is asymmetric function of mass which is flaw; the procedure to find a symmetric kernel proposed by the authors can solve this issue;
– spherical collapse model used to get an overdensity threshold seems too rough; instead were adopted the model of ellipsoidal collapse (Monaco 1997a,b) and more general non-spherical collapse model (Lee & Shandarin 1998).

Other reservations related to the environmental effects. Namely, to account to the prescripted large-scale distribution of haloes or the super-/sub-halo relation, were proposed models using considerations about merger process (Mo & White 1996, on alternatives see references therein), and also heuristic models (Peacock & Smith 2000). [1] Modifications to the Press–Schechter theory proposed in this paper allow for the presence of a host density perturbation – host halo or void, and give the mass function of sub-haloes depending on the perturbation parameters.

Below in 2nd Section we will describe a modification of the Press–Schechter theory. In 3rd Section we consider applications of the theory to superclusters and voids. Benefits and issues will be discussed in 4th Section.

## 2 PRESS–SCHECHTER THEORY WITH STATISTICAL CONSTRAINTS

### 2.1 Outline

We assume that the basic model of the theory is canonical, i.e. cumulative distribution function for variance $S$ is set by the random walk in overdensity space with variance acting as a 'time', see Bond et al. (1991) and Lacey & Cole (1993):

$$F(<S) = \mathrm{erfc}\left(\frac{\delta_*}{\sqrt{2S}}\right) , \quad (1)$$

where $\delta_*$ is the threshold overdensity for the random process, a barrier for trajectory to pierce to be associated with a collapsed object. Corresponding differential probability distribution function (PDF) is

$$f_S = \frac{\partial F(<S)}{\partial S} = \frac{\delta_*}{\sqrt{2\pi S^3}} \exp\left(-\frac{\delta_*^2}{2S}\right) . \quad (2)$$

Sheth & Tormen (1999) suggested a correction for this formula which gives better fit to their $N$-body simulations data but we will use the canonical variant for clarity. Mass PDF, $f_m$, is obtained by differentiation $F$ by mass through the mass-dependent variance. Both, threshold overdensity and variance depend on time via the

⋆ E-mail:kurbatov@inasan.ru
[1] Please excuse the author for the reference list is far from completeness. There are over 2000 citations of Press & Schechter (1974) in ADS, it's hard to analyse all of them.

cosmological model, power spectrum of fluctuations, and model of collapsing lumps. Defining these dependencies we get an evolution of the mass spectrum of haloes.

The value for threshold overdensity is commonly assumed to be $1.69$; it is obtained as a critical overdensity for collapse by considering the growth, turnaround and collapse of a uniform spherical overdense region (Bardeen et al. 1986; Lacey & Cole 1993). In general it depends on cosmological density parameters (Eke et al. 1996) but remains close to the conventional. Parameter $\delta_*$ can be interpreted not only as collapse condition but also as a marker for mass of the 'nonlinear' structures. Since the variance is the monotonic function on mass, PDF reaches its maximum value at the unique mass which sense is the characteristic or nonlinear mass, $m_*$. The extremum point for PDFs $f_S$ and $f_m$ satisfies equation $3S(m_*) = \delta_*^2$. On the other hand, in evolved systems the characteristic mass is the mass of a most frequent occurrence. As Zel'dovich et al. (1983) noted, the variance of the density grows rapidly at this mass and crosses unity, so we can reinterpet $\delta_*$ as an overdensity in objects just evolved to the nonlinear amplitude. For this we assign threshold overdensity to a value marking the characteristic mass (qualitatively the same was mentioned by Jain & Bertschinger (1994)),

$$\delta_* \equiv \sqrt{3} \approx 1.73 \; . \tag{3}$$

This value is quite close to commonly used $1.69$. Later we will assume Eq. 3 against the conventional.

Connection of the variance to the mass of the collapsed structures is implemented by filtering the local variance of density fluctuations with some kernel, which is considered isotropic usially. A space scale of the kernel, by-turn, is bound to the mass. Since fluctuations' amplitudes were small at early times, the binding is simply $m = (4\pi/3)\,\Omega_{\rm m}\rho_0 R_{\rm f}^3$, where $R_{\rm f}$ is the filtering scale, and $\Omega_{\rm m}\rho_0$ is the mean matter density in the Universe. Denote $f$ the random overdensity field. The filtered one in the real space is

$$\overline{f}(t, \boldsymbol{r}, R_{\rm W}) = \int {\rm d}^3 r'\, W(\boldsymbol{r} - \boldsymbol{r}', R_{\rm W})\, f(t, \boldsymbol{r}') \; , \tag{4}$$

where $W$ is the filter; the filtering scale $R_{\rm f}$ is bound to $R_{\rm W}$ with some filter-dependent relation, see Sect. 2.3. For the given random field the variance is

$$\begin{aligned} S &= \left\langle \left( \overline{f} - \langle \overline{f} \rangle \right)^2 \right\rangle \\ &\propto \int {\rm d}^3 k {\rm d}^3 k'\, \tilde{W}(k, R_{\rm W})\, \tilde{W}(k', R_{\rm W})\, K(t, \boldsymbol{k}, \boldsymbol{k}') \; , \end{aligned} \tag{5}$$

where $\tilde{W}$ is the Fourier image of the filtering kernel; $K(t, \boldsymbol{k}, \boldsymbol{k}') = \langle \tilde{f}(t, \boldsymbol{k})\, \tilde{f}(t, \boldsymbol{k}') \rangle$ is the correlation function for Fourier modes of unsmoothed field; the proportionality sign means free choose of a normalization constant of the Fourier transformation. The field is often assumed statistically uniform, isotropic, having zero mean and independing Fourier modes, i.e. Gaussian. This reduces the variance to depending only on isotropic power spectrum $P$ in momentum space:

$$S \propto \int {\rm d}^3 k\, \tilde{W}^2(k, R_{\rm W})\, P(t, k) \; , \tag{6}$$

where $K(t, \boldsymbol{k}, \boldsymbol{k}') = \delta_{\rm D}(\boldsymbol{k} - \boldsymbol{k}')\, P(t, k)$, i.e. modes are delta-correlated. With regard to general models, Eq. 5, if non-Gaussianity has form of the statistical constraints applied to the Gaussian field, then the correlation function can be obtained completely from power spectrum. Derivation of the correlation function in this case will be done in next Subsection.

The power spectrum itself depends on the cosmology and is represented usually in a form of the primeordial power spectrum of the given spectral index $n$ modified with transfer function $T$:

$$P(k) \propto k^n T^2(k) \; . \tag{7}$$

As an example of the transfer function can be mentioned the approximation of Bardeen et al. (1986):

$$\begin{aligned} T(k) = {} & \frac{\ln(1 + 2.34q)}{2.34q} \\ & \times \left[ 1 + 3.89q + (16.1q)^2 + (5.46q)^3 + (6.74q)^4 \right]^{-0.25} \; , \end{aligned} \tag{8}$$

where $q = k/\Gamma$, and $\Gamma$ is the shape parameter. Transfer function can also be computed numerically as the result of the evolution of perturbations in an early times, e.g. by CMBFAST code (Seljak & Zaldarriaga 1996). The unconstrained variance calculated for this power spectrum then must be normalized to the given value of $\sigma_8^2 \equiv S(R_{\rm f} = 8\,h^{-1}{\rm Mpc})$.

Calculations for evolution of the power spectrum is a difficult task even in the lowest orders of the perturbation series approach. For Gaussian field these calculations were completed just up to 1-loop corrections, i.e. to 2-nd order of accuracy in power spectrum (Jain & Bertschinger 1994), or up to 3-nd order in expressions for filtered statistical momenta (Scoccimarro 1998). In a non-Gaussian case the task became more complicated since the field is not zero-mean, and the same precision order requires much more integrals to get (Crocce & Scoccimarro 2006b,a). In our theory we will restrict ourselves to a purely linear evolution, so the overdensity will be proportional to the linear growth factor $D(t)$:

$$\begin{aligned} \overline{f}(t) &= D(t)\, \overline{f}_{\rm L} \; , \qquad P(t) = D^2(t)\, P_{\rm L} \; , \\ K(t) &= D^2(t)\, K_{\rm L} \; , \quad S(t) = D^2(t)\, S_{\rm L} \; , \end{aligned} \tag{9}$$

where L index means values linearly evolved to the present time with unity growth factor.

The linear evolution of perturbations settled on a large scale host overdensity (of both signs) can be represented in a linear perturbation theory for the certain cosmology. Parameters of such a pseudo-cosmological model determined by the mean density of the host: an overdensed background corresponds to higher value of the matter density parameter in the pseudo-cosmology than in the Universe, and vise versa. In the overdense host the perturbations will attain higher amplitudes than in global cosmology, in the underdense one the last will be lower. Since $D$ is the only factor providing the time dependency in the class of the Press–Schechter theories, the bigger values of it will be in charge of the greater age of objects population. As the population evolves mainly by merging of the objects, there is a natural connection between the host overdensity and the intensity of a merging process for sub-haloes of different mass. At this step we should obtain the bias factor for the halo number.

The result of the theory should be the number density of objects of a given mass in a predefined host halo, and also secondary values like cumulative mass of a population, etc. The number density per unit mass interval is usually defined as $\partial n_m/\partial m = \Omega_{\rm m}\rho_0 f_m/m$. In this definition is assumed the spatial homogenity of the distribution, i.e. there is no spatial structure inside the host perturbation. It might not be so in a virialized host halo, where the merger process and therefore the mass function can be affected by the sharp features of the distribution. This may lead to a mass segregation of sub-haloes in space and, hence, to redistribution of the mass spectrum of sub-haloes. We assume this feature can be modelled by a mass-dependent factor $\omega_m$, so the general definition for

the number density is

$$\frac{\partial n_m}{\partial m} = \frac{\Omega_{\rm m}\rho_0}{m}\,\omega_m f_m \ . \tag{10}$$

Factor $\omega_m$ obviously makes a contribution to the bias factor. Other distribution functions should be represented similarly.

In this work the ΛCDM model is used with following parameters: $\Omega_\Lambda = 0.7$, $\Omega_{\rm m} = 0.3$, $\sigma_8 = 0.9$, spectral index for power spectrum is $n = 1$. The transfer function was computed using the CMBFAST code of Seljak & Zaldarriaga (1996). The units adopted are $h^{-1}{\rm M}_\odot$ for mass, $h^{-1}$Mpc for length and $(hH_{100})^{-1}$ for time.

### 2.2 Constrained correlation function for modes

We represent the host halo in terms of a functional constraints for a random field of the overdensity perturbations. In our task it's convenient to make calculations using spherical modes decomposition. To obtain the correlation function for amplitudes of the spherical modes we will use the approach of Hoffman & Ribak (1992), which was proposed by them for plane waves.

The field $f(\boldsymbol{r}) = f(r,\theta,\phi)$ can be transformed to spherical modes via the transformation

$$f(\boldsymbol{r}) = \sqrt{\frac{2}{\pi}}\sum_{l=0}^{\infty}\sum_{m=-l}^{l}\int_0^\infty {\rm d}k\, kj_l(kr)Y_{lm}(\theta,\phi)\tilde{f}_{lm}(k)\ , \tag{11}$$

where $j_l$ is the radial Bessel's functions, $Y_{lm}$ is the spherical functions with normalization $\oint_{4\pi}{\rm d}\Omega\, Y^*_{lm}Y_{l'm'} = \delta_{ll'}\delta_{mm'}$. Amplitude of spherical decomposition of the field, or image, is

$$\tilde{f}_{lm}(k) = \sqrt{\frac{2}{\pi}}\int_0^\infty {\rm d}r\, r^2 kj_l(kr)\oint_{4\pi}{\rm d}\Omega\, Y^*_{lm}(\theta,\phi)f(\boldsymbol{r})\ . \tag{12}$$

Transformation for radially symmetric field $H(r)$ consists of only the isotropic modes:

$$\tilde{H}_{lm}(k) = \delta_{l0}\delta_{m0}\tilde{H}(k)\ , \tag{13}$$

where $\delta_{ij}$ is the Kronecker's delta, and

$$\tilde{H}(k) = \sqrt{4\pi}\sqrt{\frac{2}{\pi}}\int_0^\infty {\rm d}r\, r^2 kj_0(kr)H(r)\ , \tag{14}$$

while

$$H(r) = \frac{1}{\sqrt{4\pi}}\sqrt{\frac{2}{\pi}}\int_0^\infty {\rm d}k\, kj_0(kr)\tilde{H}(k)\ . \tag{15}$$

Let us write constrains in a form of linear functionals fixing up a value of the convolved field at a point. Since the local extremum is the only constraint we use, we adopt the radially symmetric constraining kernel, and place the point at origin. Using this conditions, the functional for $\alpha$-th constraint can be written in form

$$C_\alpha[f] = \int {\rm d}^3 r\, H_{(\alpha)}(r)\, f(\boldsymbol{r}) = \int_0^\infty {\rm d}k\, \tilde{H}_{(\alpha)}(k)\tilde{f}_{00}(k)\ . \tag{16}$$

Constraints itself are fixed by assigning values to these functionals. Actually kernels can depend on a set of parameters characterizing a host halo, like a space scale or some momenta. We will not write them as arguments for shortness till next Subsection.

Following Hoffman & Ribak (1991, 1992) it can be showed that the pair correlation function for the constrained ensemble of modes is

$$\begin{aligned} K_{lml'm'}(k,k') &= \left\langle \tilde{f}_{lm}(k)\tilde{f}_{l'm'}(k')\middle|\{C_\alpha\}\right\rangle \\ &= \left\langle \left(\tilde{f}_{lm}(k) - \tilde{f}^{\rm (c)}_{lm}(k)\right)\left(\tilde{f}_{l'm'}(k') - \tilde{f}^{\rm (c)}_{l'm'}(k')\right)\right\rangle\ , \end{aligned} \tag{17}$$

where the averaging performed over the unconstrained ensemble. Here

$$\tilde{f}^{\rm (c)}_{lm}(k) = \delta_{l0}\delta_{m0}Q^{-1}_{\alpha\beta}\,C_\alpha[f]\,\tilde{\Xi}_{(\beta)}(k) \tag{18}$$

is the image of the mean constrained field but with non-fixed functionals $C_\alpha[f]$; $\tilde{\Xi}_{(\alpha)}(k)$ is the image of cross-correlation function between the field and $\alpha$-th constraint:

$$\Xi_{(\alpha)}(\boldsymbol{r}) = \langle f\, C_\alpha[f]\rangle\ , \qquad \tilde{\Xi}_{(\alpha)}(k) = \tilde{H}_{(\alpha)}(k)\,P(k)\ ; \tag{19}$$

and $Q^{-1}_{\alpha\beta}$ is the inversion of the constraints correlation matrix:

$$Q_{\alpha\beta} = \langle C_\alpha[f]\,C_\beta[f]\rangle = \int {\rm d}k\,\tilde{H}_{(\alpha)}(k)\,\tilde{H}_{(\beta)}(k)\,P(k)\ . \tag{20}$$

The unconstrained field is delta-correlated, which means

$$\langle \tilde{f}_{lm}(k)\,\tilde{f}_{l'm'}(k')\rangle = \delta_{ll'}\delta_{mm'}\delta^{(1)}_{\rm D}(k-k')\,P(k)\ , \tag{21}$$

where $\delta^{(1)}_{\rm D}$ is the one-dimensional Dirac's delta-function. Our goal is to find the variance of the constrained field, i.e. the full convolution of a kind Eq. 5 for correlation function $K_{lml'm'}(k,k')$ with a filter $\tilde{W}$. It's easy to show that the only part of last meaning is

$$K(k,k') = \delta^{(1)}_{\rm D}(k-k')\,P(k) - Q^{-1}_{\alpha\beta}\,\tilde{\Xi}_{(\alpha)}(k)\,\tilde{\Xi}_{(\beta)}(k')\ . \tag{22}$$

The filtered variance can finally be expressed as

$$S = \int {\rm d}k{\rm d}k'\,\tilde{W}(k,R_{\rm W})\,\tilde{W}(k',R_{\rm W})\,K(k,k')\ . \tag{23}$$

Note that unfiltered convolution implies using the image for three-dimensional Dirac's delta-function as a filter, $\tilde{\delta}^{(3)}_{\rm D}(k) = k/(2^{1/2}\pi)$. In general, the filter can be written in the form $\tilde{W}(k,R_{\rm W}) = \tilde{\delta}^{(3)}_{\rm D}(k)\,w(kR_{\rm W})$, where $w(0) = 1$, $w(\infty) = 0$, and $0 \leqslant |w| \leqslant 1$. The same applies to the constraining kernel. This is the result of the definition for unconstrained correlator, Eq. 21, where the one-dimensional Dirac's delta-function is used. Let's set a single constraint whose kernel is the filtering kernel also, and the constraint's parameter is a space scale $R_{\rm H}$. The variance is then

$$\begin{aligned} S = \int {\rm d}k\,\Pi(k,R_{\rm W},R_{\rm W}) \\ \times\left[1 - \frac{\tilde{W}(k,R_{\rm H})}{\tilde{W}(k,R_{\rm W})}\,\frac{\int {\rm d}k'\,\Pi(k',R_{\rm W},R_{\rm H})}{\int {\rm d}k''\,\Pi(k'',R_{\rm H},R_{\rm H})}\right]\ , \end{aligned} \tag{24}$$

where $\Pi(k,R_{\rm W},R_{\rm H}) = \tilde{W}(k,R_{\rm W})\,\tilde{W}(k,R_{\rm H})\,P(k)$. It is obvious that the expression in braces tend to the values close to unity when $R_{\rm W} \ll R_{\rm H}$ or $R_{\rm W} \gg R_{\rm H}$, and vanish if $R_{\rm W} = R_{\rm H}$. Therefore, we can expect, in general, that the abundance of the haloes vanishes if halo mass tends to the mass of the host perturbation, and came closer to its unconstrained value if halo mass a lot differs from the host mass. It is not surprising.

The spatial halo correlation function is

$$\xi(\boldsymbol{r}) = \left\langle f(0)f(\boldsymbol{r})\middle|\{C_\alpha\}\right\rangle \tag{25}$$

$$\begin{aligned} &= \sqrt{4\pi}\sum_{lm}\int {\rm d}k\,\tilde{\delta}^{(3)}_{\rm D}(k)j_l(kr)Y_{lm}(\theta,\phi) \\ &\qquad\times\int {\rm d}k'\,\tilde{\delta}^{(3)}_{\rm D}(k')K_{lm00}(k,k')\ . \end{aligned} \tag{26}$$

For a spherically symmetric consraints it's image is

$$\tilde{\xi}(k) = \tilde{\delta}^{(3)}_{\rm D}(k)\,P(k) - Q^{-1}_{\alpha\beta}\,\tilde{\Xi}_{(\alpha)}(k)\int {\rm d}k'\,\tilde{\delta}^{(3)}_{\rm D}(k')\,\tilde{\Xi}_{(\beta)}(k')\ . \tag{27}$$

Time dependence of the variance and correlation function is determined by assuming linear growth, Eq. 9, i.e. by renormalization of the variance with the $D^2$ factor (see Subsection 2.4).

### 2.3 Constraining and filtering kernels

Let $H(r)$ be the kernel for the functional constraining peak (or dip) amplitude of a field at origin. Besides amplitude, the shape can be constrained also via derivations of the kernel:

$$H_{(\text{1st deriv})}(r) = \frac{\mathrm{d}H(r)}{\mathrm{d}r} \ , \quad H_{(\text{2nd deriv})}(r) = \frac{\mathrm{d}^2H(r)}{\mathrm{d}r^2} \tag{28}$$

and so on. Using reccurence relations for radial functions $j_l$ and their derivations it's easy to show that constraints for odd-order radial derivations turn to zero because of symmetry. Images for the second and fourth derivations are expressed as

$$\tilde{H}_{(\text{2nd deriv})}(k) = -\frac{k^2}{3}\,\tilde{H}(k) \ , \quad \tilde{H}_{(\text{4th deriv})}(k) = \frac{k^4}{5}\,\tilde{H}(k) \ . \tag{29}$$

Filtering kernels generally accepted to use are k-sharp, Top-hat and Gaussian:

– k-sharp

$$W_{\mathrm{KS}}(r, R_{\mathrm{W}}) = \frac{1}{2\pi R_{\mathrm{W}}^3}\,\frac{j_1(r/R_{\mathrm{W}})}{r/R_{\mathrm{W}}} \ , \tag{30}$$

$$\tilde{W}_{\mathrm{KS}}(k, R_{\mathrm{W}}) = \tilde{\delta}_{\mathrm{D}}^{(3)}(k)\,\theta(1 - kR_{\mathrm{W}}) \ ; \tag{31}$$

– Top-hat

$$W_{\mathrm{TH}}(r, R_{\mathrm{W}}) = \frac{3}{4\pi R_{\mathrm{W}}^3}\,\theta(1 - r/R_{\mathrm{W}}) \ , \tag{32}$$

$$\tilde{W}_{\mathrm{TH}}(k, R_{\mathrm{W}}) = \tilde{\delta}_{\mathrm{D}}^{(3)}(k)\,3\,\frac{j_1(kR_{\mathrm{W}})}{kR_{\mathrm{W}}} \ ; \tag{33}$$

– Gaussian

$$W_{\mathrm{G}}(r, R_{\mathrm{W}}) = \frac{1}{(2\pi)^{3/2} R_{\mathrm{W}}^3}\,e^{-r^2/(2R_{\mathrm{W}}^2)} \ , \tag{34}$$

$$\tilde{W}_{\mathrm{G}}(k, R_{\mathrm{W}}) = \tilde{\delta}_{\mathrm{D}}^{(3)}(k)\,e^{-k^2R_{\mathrm{W}}^2/2} \ ; \tag{35}$$

where $\tilde{\delta}_{\mathrm{D}}^{(3)}(k) = k/(2^{1/2}\pi)$ is the image of the three-dimensional Dirac's delta-function. Consider one of these kernels as the constraining kernel which depends on only the single parameter, a space scale $R_{\mathrm{H}}$. Volume integral for any of these filters is normalized to unity, although it is not necessary for constraining kernels since any factor will be reduced in Eq. 22. However, this normalization allows for clear physical treatment of constraints. For example, the mass of the host perturbation with overdensity $\Delta^{(\mathrm{c})}(r)$ inside a sphere of radius $r$ is

$$M(<r) = \int \mathrm{d}^3r'\,\rho(r')\,\theta(1 - r'/r) \tag{36}$$

$$= \frac{4\pi}{3}\,\Omega_{\mathrm{m}}\rho_0 r^3\left(1 + \int_0^\infty \mathrm{d}k\,\tilde{\Delta}^{(\mathrm{c})}(k)\,\tilde{W}_{\mathrm{TH}}(k, r)\right) \ , \tag{37}$$

where the second term in braces is the overdensity averaged in the volume of the host. The host overdensity profile can be obtained using Eq. 18 for the fixed values of the constraining functionals $C_\alpha$, then the averaged one will be

$$\overline{\Delta} = Q^{-1}_{\alpha\beta}C_\alpha \int \mathrm{d}k\,\tilde{W}_{\mathrm{TH}}(k, r)\,\tilde{H}_{(\beta)}(k, R_{\mathrm{H}})\,P(k) \ . \tag{38}$$

Relation between the characteristic scale $R_{\mathrm{W}}$ and filtering radius $R_{\mathrm{f}}$, as well as between the scale $R_{\mathrm{H}}$ and actual constraining radius $R_{\mathrm{h}}$ is determined by the choise of the kernel. As Bardeen et al. (1986) noted, the characteristic scale for the Top-hat filter is not the actual space scale which is filtered out if we interested in the mass enclosed inside, but connected to it via $R_{\mathrm{f}} = 0.64R_{\mathrm{W}}$. For this ratio and specified power spectrum normalization, $\sigma_8 = 0.9$, the nonlinear mass for unconstrained power spectrum is $m_* \approx 3 \times 10^{14}h^{-1}\mathrm{M}_\odot$. This value is used to adjust characteristic scales for k-sharp and Gaussian kernels. As a result, the ratio for k-sharp kernel as well as Gaussian is $R_{\mathrm{f}} = 1.4R_{\mathrm{W}}$. Ratio for the constraining scale is assumed the same, accordingly to the kernel used. The constraining mass is defined similarly to the filtered one: $M_{\mathrm{h}} = (4\pi/3)\,\Omega_{\mathrm{m}}\rho_0 R_{\mathrm{h}}^3$.

For the single constraint with $H = W_{\mathrm{TH}}$ we can see that the value of the constraining functional is bound to the mass associated with the host perturbation and to the averaged overdensity:

$$\overline{\Delta}(R_{\mathrm{h}}) \equiv C = \frac{3M_{\mathrm{h}}}{4\pi\Omega_{\mathrm{m}}\rho_0 R_{\mathrm{h}}^3} - 1 \tag{39}$$

(note the remark on constraining scale made in the previous paragraph). This quantity carries the growth factor of the host perturbation for a given epoch, as a multiplier.

Choice of the constraining kernel as well as filtering one is not unique and motivated by convenience usually. Top-hat kernel is a natural choice for a mass constraint as it has no 'tails' in the real space. On the other hand the k-sharp filter suits better for excursion set formalism (Bond et al. 1991). Also k-sharp kernel gives simple expressions in momentum space. Indeed, consider the single constraint with $H = W = W_{\mathrm{KS}}$. Denoting $S^{(0)}$ an unconstrained variance (Eq. 6) we get the trivial relation for subhaloes ($R_{\mathrm{W}} < R_{\mathrm{H}}$):

$$S = S^{(0)}(R_{\mathrm{W}}) - S^{(0)}(R_{\mathrm{H}}) \ . \tag{40}$$

Something similar should take place for other kernels, although in a case of a larger number of constraints it might not be so. At Fig. 1 is presented the function $S_{\mathrm{L}}(m)$ for different kernels and different numbers of constraints. The models were computed for the host halo mass $M_{\mathrm{h}} = 10^{12}h^{-1}\mathrm{M}_\odot$. As we see the Top-hat kernel lead to the variance stable with respect to adding more constraints. Also the k-sharp has the same property for masses $m < M_{\mathrm{h}}$ but it gives oscillations for greater masses, seemingly due to oscillations in the real space. In the case of the Gaussian filter we see a more logical behaviour: the increase in the number of statistical constraints lead to the decrease in the variance in total. Note, since the function $S_{\mathrm{L}}(m)$ is monotonically decreases, the lesser values of the variance cause the lesser amount of sub-haloes of associated mass, shifting mass PDF to the lower masses while the total amount of mass keeps unchanged and equals to $M_{\mathrm{h}}$. Nevertheless, the adopting of Top-hat kernel instead of k-sharp, or Gaussian instead of Top-hat lead to effectively lower host mass and to younger sub-halo population. Applying different kernels for constraint and filter is probably not a good idea since kernels may interfere giving oscillations in real space.

### 2.4 Linear growing of perturbations

A linear evolution law for density perturbations is known for an arbitrary uniform and isotropic cosmology model (Bildhauer et al. 1992). It depends on global density parameters of the Universe and gives the amplitude of decaying or growing modes as a function of scale factor or redshift. The solution for a growing mode is

$$D^{(0)} = \frac{5}{2}\,a^{-3/2}\chi(a)\int_0^a \mathrm{d}b\,\frac{b^{3/2}}{\chi^3(b)} \ , \tag{41}$$

where

$$\chi(a) = \left(1 + \frac{\Omega_{\mathrm{k}}}{\Omega_{\mathrm{m}}}\,a + \frac{\Omega_\Lambda}{\Omega_{\mathrm{m}}}\,a^3\right)^{1/2} \ . \tag{42}$$

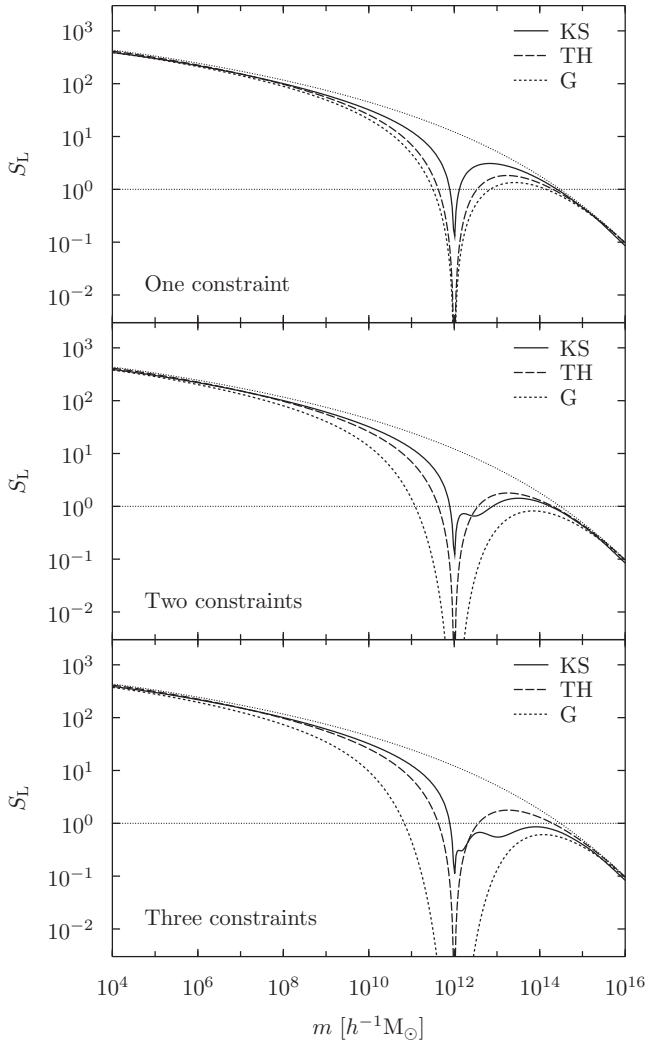


**Figure 1.** Linearly evolved variance calculated for various number of constraints, from top to bottom: one (just kernel), two (the kernel and its 2-nd derivation) and three (the kernel, its 2-nd & 4-th derivations). Host halo mass is $10^{12}h^{-1}{\rm M}_\odot$. Kernels used are: k-sharp (solid line), Top-hat (long-dashed) and Gaussian (short-dashed). Upper dotted line is the unconstrained variance, and horizontal dotted line marks the level of nonlinearity, $S_{\rm L}=1$. As seen, the Top-hat kernel gives variance which is invariant to the change of the number of constraints. For k-sharp kernel this property is true only for masses lesser than host. In both cases, the nonlinear mass is of order of the host halo mass. Using Gaussian kernel leads to the substantial dependence of the variance on the constraints number.

The evolution of perturbations inside an overdense or underdense region can be examined in a pseudo-cosmological notation, if parameters of such notation are chosen appropriately (Peebles 1993). Namely, the need to set the density of the matter and dark energy to corresponding values in a host halo or void, then do the integral for growth factor using the new density parameters:

$$\begin{aligned}\Omega'_{\rm m} &= (1+\overline{\Delta})\,\Omega_{\rm m}\\ \Omega'_\Lambda &= \Omega_\Lambda\\ \Omega'_{\rm k} &= 1-\Omega'_\Lambda-\Omega'_{\rm m}\end{aligned} \qquad (43)$$

Growth factor calculated in thise case we will denote $D$. Here $\overline{\Delta}$ is the overdensity of a host perturbation linearly evolved to the present day, i.e. using the notation of Eq. 9, it can be written as $D^{(0)}(z=0)\,\overline{\Delta}_{\rm L}$. It is natural to bind this value to the overdensity

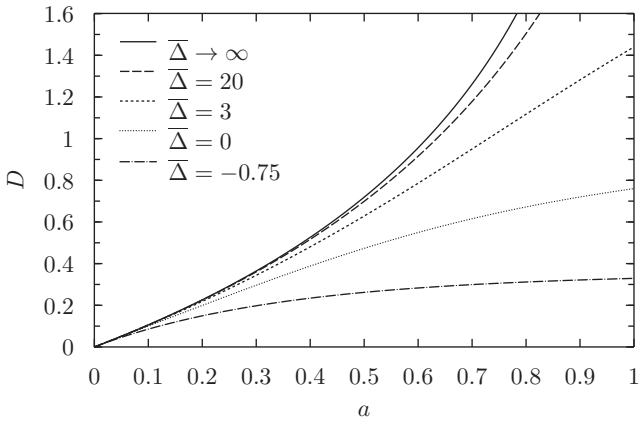


**Figure 2.** Linear growth factor as the function of scale factor. Perturbations are settled on a background with different overdensity $\overline{\Delta}$. The case $\overline{\Delta}=0$ corresponds to the unperturbed background. The solid line is the upper limit of the dependence when $D(z=0)=5$ (see text).

averaged over the volume of the host perturbation, Eq. 39, namely $\overline{\Delta}=\overline{\Delta}(R_{\rm h})$, understanding the last as evolved to the present time. Substituting these definitions into equations above we get a law of growth on the given background. Properties of solutions are following. If the linear overdensity of the host is positive, then the amplitude will grow faster turning to a greater value at present time. However, an arbitrarily large value of $\overline{\Delta}$ can lead to only finite linear amplitude at present time with limiting value $D(0)=5$ (Bildhauer et al. 1992, eq. 21 for $\Omega_{\rm m}\gg 1$). Otherwise, the arbitrarily small value of the linear overdensity lead to smaller values of amplitude at present time, giving $D(0)=0$ as a limiting case for $\overline{\Delta}=-1$.

## 3 APPLICATIONS

Our theory involves several parameters in addition to those in the original Press–Schechter approach. The parameters are the spatial scale of constraints $R_{\rm h}$ or associated mass $M_{\rm h}$, and the mean overdensity $\overline{\Delta}$. Constraining kernel can also be chosen fairly free. As we seen in Subsec. 2.3 the, different kernels with the same spatial scale effectively correspond to the different masses of the host halo, since they give different rates of decrease of the variance with spatial scale. Such an effective mass or scale can be used to calibrate $R_{\rm h}$ for various kernels. The effective value of this parameter can be calculated as the spatial momentum of $\Delta^{(\rm c)}(r)$ profile or so. Other way is to bind the effective scale to the scale where constrained variance crosses unity. Seems reasonable to use the model with $H=W=W_{\rm TH}$ as a reference because the relations of the kind Eq. 39 looks naturally in the real space for this case. In the following examples of applications we'll use the Top-hat kernel both for filter and for constraints.

We need to check the correctness of our theory for various types of the real objects. As was mentioned in Subsec. 2.1, the structure of the host halo may affect the mass function of the sub-halo population. This impact should take place through the mass segregation and to be reflected in the sub-halo merging process. It is reliably enough to assume that such situation occurs in virialized haloes only. Hence, the knowingly non-virialized structures such as voids and friable superclusters, having low overdensities ($\overline{\Delta}\ll 100$, see Lacey & Cole (1993)), are free from this effect of the 'structure biasing'. Last means that for these objects the $\omega_m$

factor in Eq. 10 equals to unity and number density PDF becomes

$$\frac{\partial n_m}{\partial m} = \frac{\Omega_{\rm m}\rho_0}{m}\, f_m \ , \qquad f_m = \left|\frac{\partial S}{\partial m}\right| f_S \ , \tag{44}$$

where $f_S$ from Eq. 2. The cumulative distribution function is

$$N(>m) = \int_m^{M_{\rm h}} {\rm d}m' \, \frac{M_{\rm s}}{m'}\, f'_m \ , \tag{45}$$

where $M_{\rm s}$ is the total mass of an area of interest, i.e. of the sub-area of a supercluster or void. This value can be bound to the observed scale $R_{\rm s}$ at the given redshift via relation $M_{\rm s} = (4\pi/3)\,\Omega_{\rm m}\rho_0 R_{\rm s}^3(1+\overline{\Delta})$. Without resorting to calculations we can find qualitative properties of these distributions. Since the growth factor is limited for all possible values of the host overdensity, and the variance depends on the mass continuously (if constraining kernels are continuous), there are the limiting distribution finction for given constraining scale $R_{\rm h}$ or $M_{\rm h}$, corresponding to the limit of the evolution of sub-haloes population when the high-mass end of the PDF is the heaviest possible. Other limiting property is the low-mass end of the distribution where PDF tends to the unconstrained law which is rescaled accordingly to the growth factor value and independent of $M_{\rm h}$.

Below we will very briefly touch three possible applications of the theory: the mass function in superclusters and also in the voids, and the bias relation for haloes in non-virialized hosts. The primary goal here to show the dependence of the distribution functions on the host overdensity.

### 3.1 Superclusters

Superclusters exhibit a very broad distribution of sizes from $10h^{-1}$ Mpc extending up to $150h^{-1}$ Mpc, and mass up to $10^{16}h^{-1}{\rm M}_\odot$. These objects form mainly in shells and filaments, although lumps are also observed. Clusters of galaxies are the characteristic components of superclusters. The typical dynamical mass of rich clusters is about $10^{13} - 10^{15}h^{-1}{\rm M}_\odot$. A number of rich clusters in supercluster can vary from several to over ten, and their mass fraction can be about 50 per cent (Bahcall 1999).

Superclusters can be characterized with density enhancement factor which is the number of objects (clusters or galaxies) in the supercluster related to the mean number of objects in the same volume (Bahcall & Soneira 1984). On the theoretical base the factor can be represented as the relation

$$E = \frac{N(<m)}{N^{(0)}(<m)}\,(1+\overline{\Delta}) \ , \tag{46}$$

where $m$ is the lowest mass of objects we are counting. Here the Eq. 45 is used with $M_{\rm s} = M_{\rm h}$, and the factor $1+\overline{\Delta}$ is applied to transform the Lagrange volume of the evolved host perturbation to the unperturbed Eulerian one. The density enhancement factor keeps information about total mass or radius and depth of the host perturbation. On the Fig. 3 this function is presented for $M_{\rm h} = 10^{15}$ and $10^{16}h^{-1}{\rm M}_\odot$, and for various overdensity values. In the low-mass limit ($m \lesssim 10^{10}h^{-1}{\rm M}_\odot$, which corresponds to the dwarf galaxies) the density enhancement factor reduces to dependence on $\overline{\Delta}$ only,

$$E \approx \frac{D^{(0)}}{D}\,(1+\overline{\Delta}) \ , \tag{47}$$

so measuring $E$ by counting objects of small masses we can restore profile of the host overdensity. However, this may be difficult since the number of dwarf galaxies in a superscuster can be tens and hundreds of thousands, and it may be biased by a sub-clustering. In order to obtain the density profile by counting objects of moderate masses the following way might be used. Considering an external radius of a supercluster $R_{\rm s}$, count the number and the density enhancement factor of objects having mass greater than some value. Then solve Eqs 45 and 46 assuming $M_{\rm s}$ corresponding to $R_{\rm s}$ (see the prevoius Subsec.). Solving equations we get the mean overdensity $\overline{\Delta}$ and the lowest mass used previously for counting, i.e. it is possible to calibrate the assumed lowest mass. The parameters found can be used further for smaller radii.

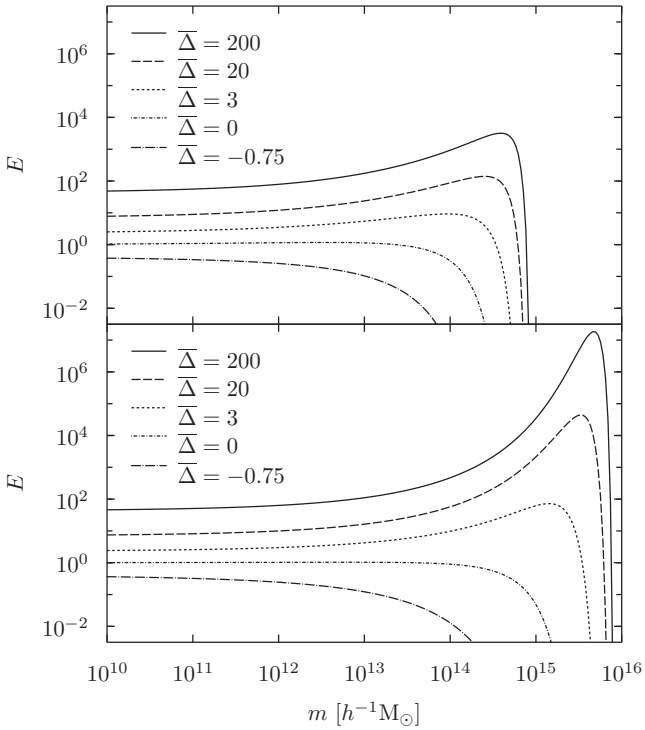


**Figure 3.** Density enhancement factor as the function of the lowest sub-halo mass used for counting, and the host overdensity. Top panel: $M_{\rm s} = M_{\rm h} = 10^{15}h^{-1}{\rm M}_\odot$. Bottom panel: $M_{\rm s} = M_{\rm h} = 10^{16}h^{-1}{\rm M}_\odot$. As seen, there is no dependense of the factor on the host halo mass or on the lowest sub-halo mass for small values of last, although the dependense is strong for moderate and high masses. In theory with unconstrained statistics we have $E \equiv 1$ (not shown).

Example of cumulative mass functions for the host $M_{\rm h} = 10^{16}h^{-1}{\rm M}_\odot$ is shown at Fig. 4. We see that the mass of the most massive sub-halo (level $N = 1$) increases several times when overdensity changes from 3 to 20 but does not become higher than $\sim 20$ per cent of the mass of host. On these figures and on the graph of the cumulative mass fraction of sub-population (Fig. 5) is seen how the distribution of sub-halo masses slides toward the high mass end when increasing host overdensity. This bias will be examined more detailed in Subsec. 3.3.

### 3.2 Voids

Voids are formed from an underdensed regions by ousting the matter out and building the cosmological walls herewith. Voids are characterized by the typical size of tens megaparsecs and prolate shape (Foster & Nelson 2009). According to simulations, the overdensity of the matter inside a void can be as low as $-0.95$ at Hubble time (van de Weygaert & van Kampen 1993).

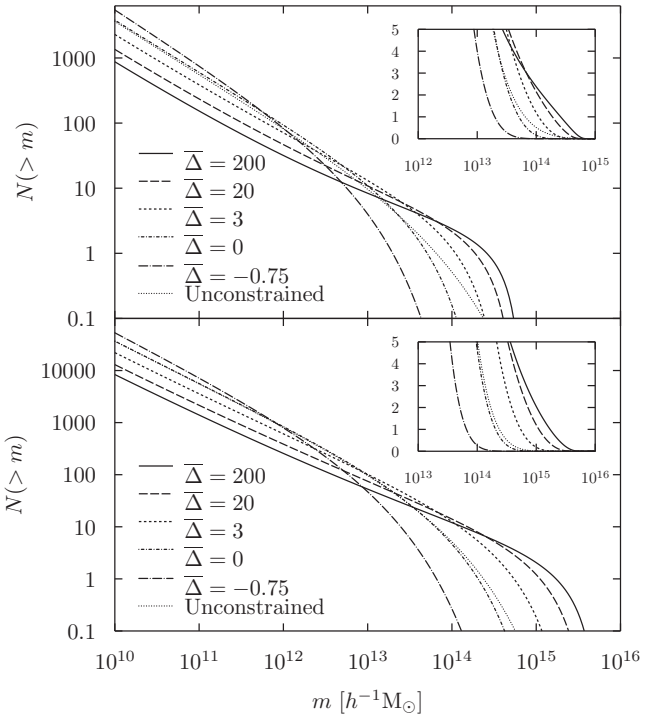


**Figure 4.** Cumulative distribution functions for sub-haloes inside a host. Top panel: $M_\mathrm{s} = M_\mathrm{h} = 10^{15}h^{-1}\mathrm{M}_\odot$. Bottom panel: $M_\mathrm{s} = M_\mathrm{h} = 10^{16}h^{-1}\mathrm{M}_\odot$. The increment of the overdensity induces the redistribution of the mass function to higher mass values. Inset shows the same graphs zoomed in the high-mass end. The mass function for unconstrained case is very close to the case $\overline{\Delta} = 0$, as expected.

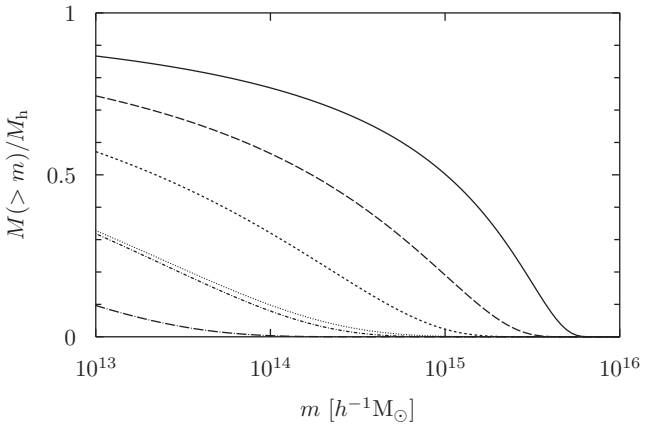


**Figure 5.** Cumulative distribution function of the mass fraction of sub-haloes inside a host $M_\mathrm{s} = M_\mathrm{h} = 10^{16}h^{-1}\mathrm{M}_\odot$ for various linear overdensities. Designations of overdensities by lines are the same as in Fig. 4.

Pustilnik & Tepliakova (2011) showed that galaxies in the Lynx-Cancer void can form groups and filaments. So the sub-halo population in voids is not spatially smooth but undergoes clustering. The distribution functions of sub-halo population inside voids are represented on Figs. 4, 5 and 6 for $\overline{\Delta} = -0.75$.

Despite the fact that cosmological voids don't virialize they become nonlinear and the void's boundaries become walls, so the total amount of mass occupied by the structure distinguished as a void is by few orders smaller than mass of the host perturbation. As the mean overdensity in a void is negative, the sub-halo

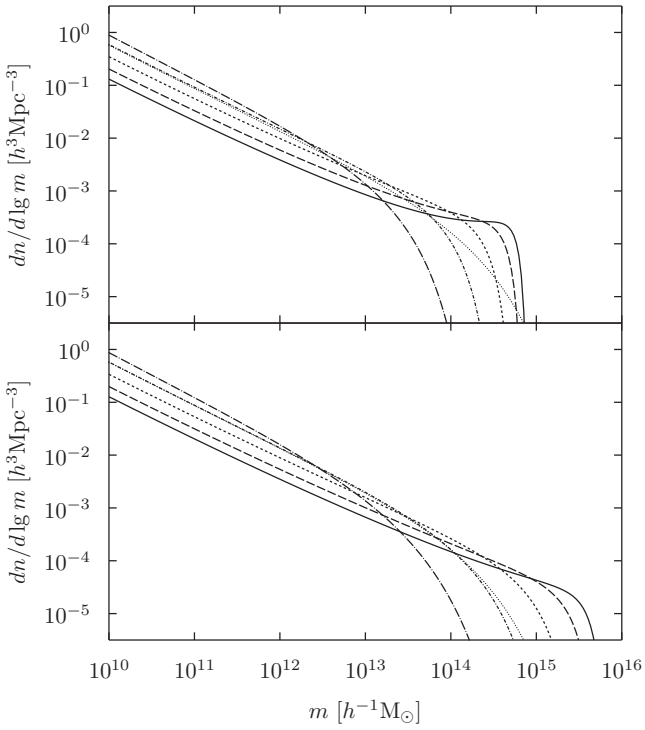


**Figure 6.** Distribution function of the number density of sub-haloes inside a host. Top panel: $M_\mathrm{h} = 10^{15}h^{-1}\mathrm{M}_\odot$. Bottom panel: $M_\mathrm{h} = 10^{16}h^{-1}\mathrm{M}_\odot$. Designations of overdensities by lines are the same as in Fig. 4.

population should be younger comparing to the supercluster or to the unconstrained case, i.e. the mass function should be heavier in the low-mass end. For these reasons the deficit of massive galaxies should be observed leading to sharper decay of the luminosity function for galaxies of moderate and high masses. This may be seen clearer on the number density distribution function, Fig. 6. Comparing to the original Press–Schechter theory without constraints (dotted line) the PDF inside the void (long-dash-dotted line) has more sharp decline, so the differents become significant for $m > 10^{12}h^{-1}\mathrm{M}_\odot$. Pustilnik & Tepliakova (2011) didn't observe this effect for their Lynx-Cancer void galaxies sample. This can be explained by the fact that the sample is limited by the absolute magnitude $\sim -18$ which corresponds to dwarf galaxies having photometric mass $M_{25} \sim 10^{10}\mathrm{M}_\odot$ (Karachentsev et al. 2004, the Hubble parameter is $h = 0.72$), so the halo mass doesn't exceed $10^{11}\mathrm{M}_\odot$. This mass limit reveals the trivial behaviour of the low-mass end of mass function (Fig. 6). To distinguish the features our theory brings, the galaxies with absolute magnitude lesser than $-20$ or $M_{25} \gtrsim 10^{11}\mathrm{M}_\odot$ should be observed. For example, if the host perturbation has the mass of order $M_\mathrm{h} \sim 10^{16}h^{-1}\mathrm{M}_\odot$ and the mean overdensity of the void is $\overline{\Delta} = -0.75$ inside the sphere $R_\mathrm{s} = 15h^{-1}$ Mpc (see simulations of van de Weygaert & van Kampen (1993)), then the enclosed mass is $M_\mathrm{s} \sim 10^{14}h^{-1}\mathrm{M}_\odot$. Such void should contain a few haloes of mass $\sim 10^{12}h^{-1}\mathrm{M}_\odot$.

### 3.3 Bias factor

Galaxy biasing is known effect when the bright galaxies tend to form near the high density peaks (Bardeen et al. 1986). In the dark matter section this property reflects the fact that density peaks are more clustered than underlying mass (Mo & White 1996). In other

words, the dark haloes trace the features of the background density field. Halo biasing was examined theoretically first by Bardeen et al. (1986). On base of the Press–Schechter theory the bias was obtained first by Mo & White (1996) as a relation between correlation functions of haloes and mass. Their expression was then extended by Sheth & Tormen (1999), revised by Jing (1998) and Porciani et al. (1999), as well adjusted with numerical N-body results.

In approach of Sheth & Tormen (1999) the Eulerian bias factor was defined as the linear part of the relative overabundance of the halo number inside volume $V$ containing given mass $M$ from the mean halo number in the same volume:

$$\delta_{\rm hh} = \frac{N(m|M,V)}{n^{(0)}(m)V} - 1 = b^{\rm PS}\overline{\Delta} + \mathcal{O}(\overline{\Delta}^2) \ , \tag{48}$$

Present day value of the factor obtained in the Press–Schechter theory is

$$b^{\rm PS} = 1 + \frac{\delta_*}{D^{(0)}S_{\rm L}^{(0)}} - \frac{D^{(0)}}{\delta_*} \ . \tag{49}$$

Jing (1998) and Porciani et al. (1999) faced the good agreement between this function and accurate numerical measurements for large halo masses, but found a departure when the mass of the halo is small; the model of Mo and White underestimated biasing for lower mass limit leading to a constant value of the bias factor while numerical measurements revealed a rising of it with mass decreasing.

The bias factor of a kind Eq. 49 depends on mass of the halo but not on the background. In the previous numerical works the procedure of calculating bias was constructed in such a way that the factor was determined being averaged on a big enough computational volume. Using formulation of the mass function proposed in this paper we can estimate the biasing effect stipulated by only the host halo mass and overdensity. In a manner Eq. 48 the relative overabundance of the halo number can be written as

$$\delta_{\rm hh} = \frac{f_m(m, M_{\rm h}, \overline{\Delta})}{f_m^{(0)}(m)}\,(1+\overline{\Delta}) - 1 \ , \tag{50}$$

where the volume tranformation factor $1+\overline{\Delta}$ is considered, and 'zero' index means the analogous values from the unconstrained theory. Eulerian bias factor then defined as

$$b \equiv \frac{{\rm d}\delta_{\rm hh}}{{\rm d}\overline{\Delta}} \ . \tag{51}$$

In this formulation both the dynamical age of the sub-halo population (determined by host overdensity $\overline{\Delta}$) and power spectrum constraints (determined by host mass $M_{\rm h}$) affect the bias. On the Fig. 7 presented the bias factor for $M_{\rm h} = 10^{16}h^{-1}{\rm M}_\odot$ and various host overdensities. The more rarefied background hosts younger sub-halo population which becomes more biased in a lower masses. At the same time the dense background demonstrates very strong biasing in a high masses comparing to the approximating formula of Mo & White. This discrepancy may be cleaned by the following way. The large scale structures of different overdensities have the different volume filling factor in the Universe. Namely, voids having negative overdensity occupy the major part of the Universe while the walls, filaments and other structures having positive overdensity occupy the volume with factor of order few per cents. Considering this it may be possible to match the rising low-mass limit of the bias (Jing 1998) while to attenuate an exponential growth of the bias factor in the high-mass limit.

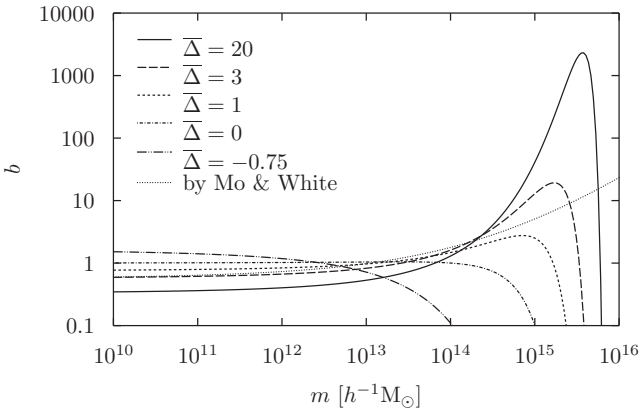


**Figure 7.** Present day Eulerian bias factor for $M_{\rm h} = 10^{16}h^{-1}{\rm M}_\odot$ and various host overdensities. It is seen, the younger sub-halo population ($\overline{\Delta}$ is lower), the more it is biased for the lower masses of sub-haloes. Dotted line shows the bias factor by Mo & White (1996).

## 4 DISCUSSION

Comparing with the original Press–Schechter theory, our theoretical model has additional parameters: mean overdensity of the host perturbation $\overline{\Delta}$, its spatial scale $R_{\rm h}$, constraining kernel $H$ defining profile of the host perturbation, and its spatial momenta $C_\alpha$, first of which is $\overline{\Delta}$. From the original theory, our approach is formally characterized in using of different mass–variance function and assuming some different background cosmology. Thereby, all the statistics it gives is spatially uniform. In addition, neither host perturbation profile nor its overdensity changes the merging process of the sub-halo population. That is, our theory in its present form is not able to model properly the virialized haloes, e.g. haloes of galaxies and galaxy clusters. As was mentioned above, the virialization process may result in mass segregation which alternates the merger rates for low- and-high-mass sub-haloes. The process has more significant influence on the high-mass end of the distribution function. This effect can be named the 'structure biasing'.

Correction to the distribution functions accounting to the structure biasing may have form of the multiplier, like in Eq. 10, depending on parameters noted above, and also on sub-halo mass. It is possible to estimate the high-mass limit of this multiplier using virial considerations. In general case the spatial distribution of the density per unit mass interval is

$$\frac{\partial\rho_m}{\partial m} = \Omega_{\rm m}\rho_0\omega f_m \ , \tag{52}$$

where $\omega = \omega(r,m)$ is a factor responding for the structure bias. Cumulative mass of a sub-halo population inside a sphere $r$ is

$$\begin{aligned} M(<r) &= 4\pi\int_0^r {\rm d}r'\,r'^2\int_0^{M_{\rm h}} {\rm d}m\,\frac{\partial\rho_m(r',m)}{\partial m} \\ &= 3M_{\rm h}\int_0^{r/R_{\rm h}} {\rm d}x\,x^2\int_0^{M_{\rm h}} {\rm d}m\,\omega f_m \ , \end{aligned} \tag{53}$$

where $x = r/R_{\rm h}$ is introduced. The $\omega$ factor depends on the virialization process and reflects as density profile of a host halo so the sub-haloes mass segregation inside it. Without going into details of virialization we can denote that sub-haloes of high mass locate naturally near the centre while low-mass haloes occupy the entire host volume. The meaning of $\omega$ then might be the relative volume filled by sub-haloes of a given mass. The factor should decrease with sub-halo mass increasing, from a constant value of order unity or greater, for $m \ll M_{\rm h}$, to a somewhat small value in the limit

$m \to M_{\rm h}$. The detailed structure of the high mass limit can be examined as follows. For definiteness let the virialized host halo has NFW density profile (Navarro et al. 1997):

$$\rho_{\rm NFW} = \frac{\Delta_{\rm c}\rho_0}{(1+r/r_{\rm s})^2\, r/r_{\rm s}} \ , \tag{54}$$

where $r_{\rm s}$ is the scale radius; $\Delta_{\rm c}$ is the characteristic overdensity. The mass profile with it's Taylor expansion is

$$\begin{aligned} M_{\rm NFW}(<r) &= M_{\rm h}\,\frac{3\Delta_{\rm c}}{200c^3}\left(\ln(1+r/r_{\rm s}) - \frac{r/r_{\rm s}}{1+r/r_{\rm s}}\right) \\ &= M_{\rm h}\,\frac{3\Delta_{\rm c}}{200c^3}\left(\frac{r^2}{2r_{\rm s}^2} + \mathcal{O}\left(\frac{r^3}{r_{\rm s}^3}\right)\right) \ , \end{aligned} \tag{55}$$

where $c$ is the concentration factor, and $M_{\rm h}$ has the meaning of the mass inside a sphere with overdensity 200, i.e. $M_{\rm h} = (4\pi/3)\,200\rho_0 r_{200}^3$, $\Omega_{\rm m}R_{\rm h}^3 = 200r_{200}^3$, and $r_{200} = cr_{\rm s}$. In the vicinity of the centre the heavy mass sub-haloes dominate by mass so we can assume mass profile of the population (Eq. 53) and of the host halo (Eq. 55) matching there. Hence, the structure bias factor can be expressed in the form

$$\omega = \frac{\Delta_{\rm c}}{\Omega_{\rm m}}\,\frac{\omega_m}{r/r_{\rm s}} \tag{56}$$

with the natural mass conservation claim

$$\int_0^{M_{\rm h}} {\rm d}m\,\omega_m f_m = 1 \ . \tag{57}$$

The mass part $\omega_m$ of the structure bias factor can be obtained using virial theorem and equipartition. Gravitational potential of NFW halo is

$$\Phi_{\rm NFW} = -\frac{3\Delta_{\rm c}}{200c^3}\,\frac{GM_{\rm h}}{r_{\rm s}}\,\frac{\ln(1+r/r_{\rm s})}{r/r_{\rm s}} \ . \tag{58}$$

Write the virial theorem, neglecting an angular momentum of the motion, then expand the virial at the lowest radii:

$$\langle v^2\rangle = \left\langle r\,\frac{{\rm d}\Phi_{\rm NFW}}{{\rm d}r}\right\rangle \propto \left\langle \frac{r}{r_{\rm s}} + \mathcal{O}\left(\frac{r^2}{r_{\rm s}^2}\right)\right\rangle \ . \tag{59}$$

Assuming equipartition at the lowest energies, we get $\langle v^2\rangle \propto m^{-1}$, and hence $\langle r\rangle \propto m^{-1}$. Now define $\omega_m$ as the volume factor, $\omega_m \propto \langle r\rangle^3$, then

$$\omega_m \propto \frac{M_{\rm h}^3}{m^3} \quad \text{for } m \sim M_{\rm h} \ . \tag{60}$$

As we see, the structure bias factor reduces the amount of massive sub-haloes simultaneously increasing the amount of small ones.

## 5 CONCLUSION

We proposed the modification of the Press–Schechter theory of dark halo clustering. The basis of modification is the use of the statistical constraints imposed on the initial gaussian random fluctuations. Constraints has the form of the linear functionals of the fluctuations' overdensity field. Kernels of constraints determine the shape and, mainly, the spatial scale of the host perturbation which evolves to the supercluster or void. The resulting non-gaussianity of the random field leads to existing of the upper limit of mass of the sub-haloes formed inside the host perturbation. Amplitude of the perturbation also determines the age of the sub-halo population in the sense of the merging process.

Since the only spherical host perturbation is adopted in this paper we can not apply our theory to the variety of morphologies of superclusters but to the lumps only. However, it is not difficult to generalize the approach used here to an arbitrary shape of the host perturbation to the wall or filament.

Calculations show, the distribution function for sub-haloes with mass fraction $10^{-4} - 10^{-3}$ of the host and greater reveal deviations from the original Press–Schechter predictions, while deviations are negligible for lower masses so they can be expressed as a rescaling. If the host halo mass is $M_{\rm h} = 10^{15}h^{-1}{\rm M}_\odot$ and its overdensity is $\overline{\Delta} = 20$, the deviations can be detected for sub-haloes of the mass $10^{12}h^{-1}{\rm M}_\odot$ and greater. Assuming dark-to-light mass relation be 10, such haloes correspond to the galaxies having absolute magnitude $-20$ and brighter (Karachentsev et al. 2004). To check the theory in a voids' galaxies is necessary to count ones with absolute magnitudes lesser than $-20$. However, there may be only a few such galaxies inside a tens-megaparsecs void. Also using theory, it is possible to recall the density profile of the superclusters.

Approach used in this paper does not allow to predict the distribution functions in virialized haloes. However, in previous section showed, the effect of the structure biasing should compensate the shift of the distribution function inside an overdense halo toward the high masses. This can explain the good fitting of the Press–Schechter function to a wide range of observations and numerical experiments.

## REFERENCES


Bahcall N. A., 1999, in A. Dekel & J. P. Ostriker ed., Formation of Structure in the Universe Clusters and superclusters of galaxies. pp 135–+

Bahcall N. A., Soneira R. M., 1984, ApJ, 277, 27

Bardeen J. M., Bond J. R., Kaiser N., Szalay A. S., 1986, ApJ, 304, 15

Benson A. J., Kamionkowski M., Hassani S. H., 2005, MNRAS, 357, 847

Bildhauer S., Buchert T., Kasai M., 1992, A&A, 263, 23

Bond J. R., Cole S., Efstathiou G., Kaiser N., 1991, ApJ, 379, 440

Crocce M., Scoccimarro R., 2006a, Phys. Rev. D, 73, 063520

Crocce M., Scoccimarro R., 2006b, Phys. Rev. D, 73, 063519

Eke V. R., Cole S., Frenk C. S., 1996, MNRAS, 282, 263

Foster C., Nelson L. A., 2009, ApJ, 699, 1252

Hoffman Y., Ribak E., 1991, ApJ, 380, L5

Hoffman Y., Ribak E., 1992, ApJ, 384, 448

Jain B., Bertschinger E., 1994, ApJ, 431, 495

Jing Y. P., 1998, ApJ, 503, L9+

Karachentsev I. D., Karachentseva V. E., Huchtmeier W. K., Makarov D. I., 2004, AJ, 127, 2031

Lacey C., Cole S., 1993, MNRAS, 262, 627

Lee J., Shandarin S. F., 1998, ApJ, 500, 14

Mo H. J., White S. D. M., 1996, MNRAS, 282, 347

Monaco P., 1997a, MNRAS, 287, 753

Monaco P., 1997b, MNRAS, 290, 439

Navarro J. F., Frenk C. S., White S. D. M., 1997, ApJ, 490, 493

Peacock J. A., Smith R. E., 2000, MNRAS, 318, 1144

Peebles P. J. E., 1993, Principles of physical cosmology. Princeton Series in Physics, Princeton, NJ: Princeton University Press

Porciani C., Catelan P., Lacey C., 1999, ApJ, 513, L99

Press W. H., Schechter P., 1974, ApJ, 187, 425

Pustilnik S. A., Tepliakova A. L., 2011, MNRAS in press

Scoccimarro R., 1998, MNRAS, 299, 1097

Seljak U., Zaldarriaga M., 1996, ApJ, 469, 437

Sheth R. K., Tormen G., 1999, MNRAS, 308, 119

van de Weygaert R., van Kampen E., 1993, MNRAS, 263, 481
Zel'dovich Y. B., Novikov I. D., Fishbone L., Steigman G., 1983, Relativistic astrophysics, Vol. 2. The structure and evolution of the Universe. The University of Chicago Press, Chicago - London

This paper has been typeset from a TEX/ LATEX file prepared by the author.